

# Ga-NMR local susceptibility of the kagomé-based magnet $\text{SrCr}_{9p}\text{Ga}_{12-9p}\text{O}_{19}$ . A high temperature study.

L.Limot<sup>1</sup>, P.Mendels<sup>1</sup>, G.Collin<sup>2</sup>, C.Mondelli<sup>3</sup>, H.Mutka<sup>3</sup>, and N.Blanchard<sup>1</sup>

<sup>1</sup>*Laboratoire de Physique des Solides, UMR 8502, Université de Paris-Sud, 91405 Orsay, France*

<sup>2</sup>*Laboratoire Léon Brillouin, CE Saclay, CEA-CNRS, 91191, Gif-sur-Yvette, France*

<sup>3</sup>*Institut Laue-Langevin, B.P. 156, F-38042 Grenoble Cedex 9, France*

## Abstract

We report a high- $T$  Ga-NMR study in the kagomé-based antiferromagnetic compound  $\text{SrCr}_{9p}\text{Ga}_{12-9p}\text{O}_{19}$  ( $.81 \leq p \leq .96$ ), and present a refined mean-field analysis of the local NMR susceptibility of Cr frustrated moments. We find that the intralayer kagomé coupling is  $J = 86(6)$  K, and the interlayer coupling through non-kagomé Cr moments is  $J' = 69(7)$  K. The  $J'/J = 0.80(1)$  ratio confirms the common belief that the frustrated entity is a pyrochlore slab.

The kagomé-based compound  $\text{SrCr}_{9p}\text{Ga}_{12-9p}\text{O}_{19}[\text{SCGO}(p), p < 1]$  has been receiving considerable attention as a model system for geometrically frustrated physics [1]. Magnetic properties of  $\text{SCGO}(p)$  arise from Heisenberg  $\text{Cr}^{3+}$  ions ( $S = \frac{3}{2}$ ). Despite macroscopic susceptibility ( $\chi_{macro}$ ) measurements which indicate that a strong antiferromagnetic interaction couples neighboring spins ( $\Theta_{macro} \approx 500 - 600$  K), spin-spin correlation never exceeds twice the Cr–Cr distance [2]. No classical Néel long range order occurs. On the contrary,  $\text{SCGO}(p)$  continues to display Curie-Weiss behavior well below  $\Theta_{macro}$  as suggested by the linear  $T$ -dependence of  $\chi_{macro}^{-1}$ , extending mean-field predictions to an unusual temperature domain ( $T \ll \Theta_{macro}$ ).

Geometric frustration arises from interacting spins on kagomé networks. However, the crystal structure is not pure kagomé since  $\text{Cr}^{3+}$  ions occupy both kagomé [ $\text{Cr}(12k)$ ] and non-kagomé [ $\text{Cr}(2a), \text{Cr}(4f_{vi})$ ] sites, as shown in the inset of Fig.1.  $\text{Cr}(2a)$  sites link two kagomé layers. The kagomé- $\text{Cr}(2a)$ -kagomé slabs are isolated from one another by  $\text{Cr}(4f_{vi})$ – $\text{Cr}(4f_{vi})$  pairs which Lee *et al.* showed to form spin singlets with a binding energy of  $\Delta = 216$  K [3]. They also suggested that the kagomé- $\text{Cr}(2a)$ -kagomé slab may be regarded as a quasi-2D highly frustrated system, which they named pyrochlore slab. However there is a lack of experimental evidence concerning couplings which ensure this slab structure. Coupling of the two kagomé planes through  $\text{Cr}(2a)$  is not known, nor is the intralayer kagomé coupling. One way to shed light into this problem, would be a refined high- $T$  analysis of the magnetic susceptibility of Cr frustrated moments. Unfortunately this is prevented in  $\chi_{macro}$  by the fact that there are contributions from all magnetic sites, frustrated and non-frustrated. Moreover,  $\chi_{macro}$  is also sensitive to disorder as non-magnetic  $\text{Ga}^{3+}$  ions are always present on  $\text{Cr}^{3+}$  sites (the  $p = 1$  compound is not stable) [4]. As we show here, such an analysis can be done by  $^{69}\text{Ga}$  and  $^{71}\text{Ga}$  ( $I = \frac{3}{2}$ ) NMR since Ga nuclei on site  $4f$  directly probe both  $\text{Cr}(12k)$  and  $\text{Cr}(2a)$  moments (see. inset Fig.1). By varying Ga/Cr substitution from 4% to 19% ( $p = .81, .89, .96$ ), we are able to separate and identify on a firm experimental ground the substitution-related susceptibility from the intrinsic frustrated susceptibility of the slab [5,6]. We present here high- $T$  results and mean-field analysis of the slab susceptibility,

which enables us to evaluate  $J'$  and  $J$ , respectively the Cr(2a)–Cr(12k) coupling and the Cr(12k)–Cr(12k) coupling. We find  $J' = 69(7)$  K and  $J = 86(6)$  K. The  $J'/J = 0.80(1)$  ratio confirms the common belief that the frustrated entity is a pyrochlore slab.

All samples are ceramics and were synthesized by solid state reaction as detailed elsewhere [6]. Reaction products were checked by standard x-ray diffraction and refined by neutron diffraction (see Table I).  $\chi_{macro}$  yielded results in agreement with previous concentrations reported in literature ( $\Theta_{macro} = 439(22), 501(14), 608(14)$  K for  $p = .81, .89, .96$  respectively) [7].

An extended NMR analysis of the spectrum was presented in previous papers [6,8]. Three different Ga NMR sites can be resolved: Ga(4e), Ga(4f) and Ga substituted on Cr sites [Ga(sub.)]. Ga(4f) is at the heart of frustrated physics (inset Fig.1). It is exclusively coupled to Cr(12k) and Cr(2a) by a Ga–O–Cr hyperfine interaction, and is the object of the present study.

A set of spectra ranging from 150 K to 410 K were performed in a  $\sim 7$  Tesla permanent magnet. We used a  $\pi/2, \pi$  sequence with spacing  $\tau = 18 \mu s$  between pulses, and as the applied frequency was swept over a  $\sim 1$  MHz range, with a step interval of 75 kHz, spin echo signals were recorded. The overall spectrum was then obtained by summing all the spin echo Fourier transforms [9]. Another set of spectra ranging from 15 K to 200 K were obtained in a sweep field setup, i.e. by varying an external magnetic field at a constant applied frequency 40.454 MHz, and recording the integral of the spin echo signal. Again we used a conventional  $\pi/2, \pi$  sequence, but with spacing  $\tau = 28 \mu s$ .

A typical set of high- $T$  ( $T \geq 100$  K) field sweep spectra for the  $p = .96$  sample, recorded around 3 Tesla, is reported in Fig.1. In this field window two lines are unambiguously resolved. Ga(4f) is the main line and the hump at its right is Ga(sub.). The negligible contribution of Ga(sub.) to the spectrum reflects the nearly stoichiometric value of the sample. The sharp non-symmetric features of the Ga(4f) line originate from  $T$ -independent quadrupole effects ( ${}^{71}\nu_Q(4f) \simeq 2.9$  MHz,  $\eta \simeq 0$ ) related to local charge environment around the nucleus. Upon cooling the NMR line shifts to the left with respect to its zero reference

position, without any appreciable broadening. The  $T$ -dependence of the shift ( $K$ ) stems from the Ga(4*f*) magnetic environment.  $K$  provides a direct measurement of the magnetic susceptibility of the Cr(12*k*) and Cr(2*a*) ions (to be detailed below).

The temperature dependence of  $K^{-1}$  is presented in Fig.2 for all samples. The high- $T$  data ( $T \gtrsim 100$  K) follows a Curie-Weiss law as suggested by the linear variation of  $K^{-1}$ . By extrapolating  $K^{-1}$  to 0 we extract the NMR Curie-Weiss temperature ( $\Theta_{NMR}$ ). We evaluate it to be 453(50) K, 469(44) K, and 484(40) K for  $p = .84, .89, .96$  respectively, of the same order of  $\Theta_{macro}$ , but somewhat lower. The increase in  $\Theta_{NMR}$  with  $p$  reflects a better lattice coverage as one would expect from mean-field theory. Here again Curie-Weiss behavior extends well below  $\Theta_{NMR}$ . Further lowering  $T$ ,  $K$  in all samples eventually deviates from Curie-Weiss behavior, flattening and even decreasing below  $T = 40 - 50$  K. We address the reader to other publications for a detailed discussion on the low- $T$  behavior of  $K$  [5,6].

We now turn to discuss the high- $T$  behavior of  $K$  within a mean-field analysis. First we would like to point out that Cr(12*k*) and Cr(2*a*) do not have same magnetic environment. Cr(2*a*) has 6 nearest neighbors of Cr(12*k*), whereas Cr(12*k*) has 5 nearest neighbors (4 Cr(12*k*) and 1 Cr(2*a*)). Furthermore Cr(12*k*)–Cr(12*k*) coupling ( $J$ ) and Cr(12*k*)–Cr(2*a*) coupling ( $J'$ ) are a priori not the same. In these regards our mean-field analysis is similar to that performed in ferrimagnetic compounds which bear inequivalent magnetic sites.

To justify this analysis we must argue how  $J$  and  $J'$  are the only relevant couplings in the slab. A study of a series of chromium oxides indicates that the Cr-Cr interaction is dominated by direct exchange [10]. It was shown that such an interaction varies rapidly with Cr–Cr distance (and Cr–O–Cr angle), being  $\approx 0$  when  $d_{Cr-Cr} \gtrsim 3.1$  Å. Therefore only interactions between Cr(12*k*)–Cr(12*k*) ( $d_{Cr-Cr} = 2.895$  Å) and Cr(12*k*)–Cr(2*a*) ( $d_{Cr-Cr} = 2.971$  Å) are relevant in the frustrated unit, with  $0 < J' < J$ . Cr(2*a*)–Cr(2*a*) interaction is  $\approx 0$  as  $d_{Cr-Cr} = 5.80$  Å. Note that the kagomé layer is distorted, therefore  $J$  represents the average coupling between Cr(12*k*).

On the basis of these considerations, the frustrated spin Hamiltonian is

$$\mathcal{H} = J \sum_{\langle i,j \rangle} \left[ (\vec{S}_{12k})_i \cdot (\vec{S}_{12k})_j + \varepsilon (\vec{S}_{12k})_i \cdot (\vec{S}_{2a})_j \right],$$

where we have introduced  $0 < \varepsilon = J'/J < 1$ . The first term is the isotropic Heisenberg interaction between spins  $\vec{S}_{12k}$  on the kagomé layer. The second term is the interaction between  $\vec{S}_{12k}$  and  $\vec{S}_{2a}$  spins. The summation is taken over neighboring spins of the slab.

Using a mean-field approach the  $\chi_{12k}$  and  $\chi_{2a}$  susceptibilities per site of Cr(12k) and Cr(2a) can be written

$$\chi_{12k} = \frac{\mu_{eff}^2}{3k_B T f(T)} \left( 1 - \frac{p_{2a} S(S+1) \varepsilon J}{3k_B T} \right), \quad (1)$$

and

$$\chi_{2a} = \frac{\mu_{eff}^2}{3k_B T f(T)} \left( 1 + \frac{6p_{12k} S(S+1)(2/3 - \varepsilon) J}{3k_B T} \right), \quad (2)$$

where  $f(T) = 1 + 4p_{12k} S(S+1)J/3k_B T - 6p_{12k} p_{2a} (\varepsilon J S(S+1)/3k_B T)^2$ . The two expressions are different and reflect the fact that the two sites have different magnetic environments. The effective magnetic moment is  $\mu_{eff} = 3.83\mu_B$ , typical of  $S = 3/2$  Cr<sup>3+</sup> ions [11].  $p_{12k}, p_{2a}$  are the occupation of the Cr(12k) and Cr(2a) sites known from neutron refinement (cf. Table I). The only unknown parameters are  $J$  and  $\varepsilon$ . In Fig.3 we show the evolution of  $\chi_{12k}$  and  $\chi_{2a}$  when increasing  $\varepsilon$ , with a fixed value  $J$ . In the limit  $\varepsilon = 0$ ,  $\chi_{12k}$  follows a Curie-Weiss law with a kagomé Curie-Weiss temperature  $4p_{12k} J S(S+1)/3$ . Whereas  $\chi_{2a}$  follows a Curie law as we have freed the Cr(2a) spin from its magnetic environment. As  $\varepsilon$  is increased, the pure paramagnetic behavior of  $\chi_{2a}$  progressively dies out, while  $\chi_{12k}$  is little affected. Of interest is when the kagomé-Cr(2a)-kagomé slab behaves as a pyrochlore slab. By pyrochlore slab we mean that both magnetic sites are identical  $\chi_{12k} = \chi_{2a}$ , i.e.  $\varepsilon = \varepsilon_0 = 4p_{12k}/(6p_{12k} - p_{2a})$ . For an homogeneous substitution ( $p_{12k} = p_{2a} = p$ )  $\varepsilon_0 = 0.8$ , reflecting the fact that the effective exchange field on Cr(2a) ( $6J'$ ) and on Cr(12k) ( $4J + J'$ ) are then identical. We stress that this relation is independent on distortion on the kagomé layer, as it only involves the average exchange constant  $J$ .

We may express the NMR shift  $K$  using the mean-field expressions (1) and (2)

$$K \propto (9p_{12k}\chi_{12k} + 3\delta p_{2a}\chi_{2a}) \quad (3)$$

where we have introduced  $\delta = A'/A$ .  $A, A'$  are the hyperfine constants which are respectively a measurement of the Cr(12*k*),Cr(2*a*) moment at the nuclear site, and just influence the thermal behavior of  $K$  by their ratio  $\delta$ . The two terms of expression (3) are multiplied by the number of neighboring Cr(12*k*) and Cr(2*a*) linked by the oxygen ions to the Ga(4*f*) nucleus, respectively 9 and 3. We can fix a lower bond to  $\delta$  by some simple structural remarks. The hyperfine bridge Ga(4*f*)–O–Cr(12*k*) yields bond lengths of  $d_{Ga(4f)-O} = 1.866$  Å and  $d_{O-Cr(12k)} = 2.052$  Å. The hyperfine bridge Ga(4*f*)–O–Cr(2*a*) yields bond lengths of  $d_{Ga(4f)-O} = 1.866$  Å and  $d_{O-Cr(2a)} = 1.971$  Å. The small difference in length and the similarity for angles between these bonds leads to a stronger coupling to Cr(2*a*) then to Cr(12*k*), and  $\delta > 1$ . A more precise calculation suggests  $\delta \approx 2$  [8]. It is instructive to compare  $K$  to the expression of the susceptibility of the kagomé-Cr(2*a*)-kagomé slab that one would obtain from a macroscopic measurement

$$\chi_{slab} = 6p_{12k}\chi_{12k} + p_{2a}\chi_{2a}$$

where  $\chi_{12k}$  and  $\chi_{2a}$  are now weighted by 6 and 1, respectively the number of Cr(12*k*) and Cr(2*a*) per formula unit of SCGO.  $K$  is an independent measurement of the slab susceptibility, but with a different weighting than  $\chi_{slab}$ . Using  $\delta \approx 2$ , we see that  $\chi_{2a}, \chi_{12k}$  impact  $K$  in a ratio of 6/9 instead of 1/6 for  $\chi_{slab}$ .  $K$  on the contrary of  $\chi_{slab}$  is very sensitive to temperature dependence of  $\chi_{2a}$ , meaning that it is also very sensitive to  $\varepsilon$ .

The shift  $K$  reveals three unknown parameters  $J, \varepsilon$ , and  $\delta$ . Our aim is to determine their values by fitting for  $T \geq 100$  K the shift-data presented in Fig.2. There are an infinity of  $(\varepsilon, J, \delta)$ -set of values which reproduce the linear variation of  $K^{-1}$  with  $T$ . In Fig.4 we present the set of  $(\varepsilon, J, \delta)$ -values obtained when fitting  $K^{-1}$  of the  $p = .96$  sample with expression (3). As shown, for a given value of  $\varepsilon$  (abscissa) there is an associated value  $\delta$  (upper panel) and  $J$  (bottom panel). In order to seize the evolution of this set of parameters it is instructive to examine the dependence of  $\delta$  on  $\varepsilon$ . In the limit  $\varepsilon \rightarrow 0$ , we see that  $\delta \rightarrow 0$ . In fact when  $\varepsilon = 0$ ,  $\chi_{2a}$  follows a Curie law. Therefore to reproduce the linear

variation of  $K^{-1}$  there is only one possibility: uncouple the Ga( $4f$ ) nuclei from Cr( $2a$ ), setting  $\delta = 0$ . As  $\varepsilon$  is increased,  $\delta$  monotonically increases since Curie contribution from  $\chi_{2a}$  dies out. But when  $\varepsilon = \varepsilon_0$  expression (3) reduces to  $K \propto (9p_{12k} + 3\delta p_{2a})\chi_{12k}$ , since in this case  $\chi_{12k} = \chi_{2a} = \chi_{slab}/(6p_{12k} + p_{2a})$ . The  $T$ -dependence of the shift is then completely determined by the  $(\varepsilon, J)$  pair of values, whatever the value of  $\delta$ . When  $\varepsilon > \varepsilon_0$ , we recover the monotonic increase in  $\delta$ . Of interest is also the slow monotonic decrease of  $J$  with increasing  $\varepsilon$ . Since  $0 < J' < J$ , i.e.  $0 < \varepsilon < 1$ , we conclude that  $80 \text{ K} \lesssim J \lesssim 100 \text{ K}$ . However only the set of values for which  $\delta > 1$  bear a physical solution. Two possibilities subsist: (i) the set of values close to  $\varepsilon \approx \varepsilon_0$  (ii) the set of values for  $\varepsilon \gtrsim 4$ . Case (ii) is a non-physical solution. This leads us to one of our major findings: the high- $T$  linear behavior of  $K^{-1}$  reflects the physics of a pyrochlore slab, with the consequence that  $K \propto \chi_{slab}$ .

Results for all samples are presented in Table I. Errors are governed by error bars on  $p_{12k}$  and  $p_{2a}$  from neutron diffraction data. Coupling constants are found independent on lattice coverage given the negligible variation of lattice parameters with substitution. Turning to the value of  $J$ , it is very satisfying to find a coupling constant close to the one observed in Cr<sub>2</sub>O<sub>3</sub>, where Cr<sup>3+</sup> ions have a local octahedral environment ( $d_{Cr-Cr} = 2.890 \text{ \AA}$ , Cr–O–Cr = 93.1°) similar to Cr( $12k$ ) ( $d_{Cr-Cr} = 2.895 \text{ \AA}$ , Cr–O–Cr = 93.8°). There, it was established that the exchange coupling between neighboring Cr is 77(3) K [12]. We also performed a consistency test by calculating the expected values of  $\Theta_{NMR}$  using results reported in Table I. The analytical expression of  $\Theta_{NMR}$  is obtained from the high- $T$  limit ( $T \gg S(S + 1)J$ ) of expression (3). We find 456(56), 460(33) and 495(35) K for  $p = .81, .89$  and  $.96$  respectively, in agreement with experimental values of  $\Theta_{NMR}$ . Finally by using the susceptibility of Cr( $4f_{vi}$ )–Cr( $4f_{vi}$ ) pairs [3], we are able to reproduce the high- $T$   $\chi_{macro}$ –data where the susceptibility  $\chi_{slab}$  adds on to the Cr( $4f_{vi}$ ) and to the defect induced susceptibilities.

In conclusion, we have evidenced that the Curie–Weiss behavior of the frustrated slab susceptibility extends to much lower temperatures than the average Cr–Cr interaction. A high- $T$  mean-field analysis allowed us to determine couplings involved in the frustrated

physics. We confirm the common belief that frustration in  $SCGO(p)$  arises from a pyrochlore slab.

We wish to acknowledge fruitful discussions with A. Keren, C. Lhuiller, F. Mila, M. Horvatić, and B. Duçot.

$p$	$p_{12k}$	$p_{2a}$	$p_{4f_{vi}}$	$J$ (K)	$\varepsilon$
.81(1)	.79(1)	.95(2)	.81(1)	94(9)	.82(2)
.89(1)	.89(1)	.94(2)	.86(1)	85(6)	.81(2)
.96(1)	.96(1)	1.00(2)	.94(1)	86(6)	0.80(1)

TABLE I. Nominal occupation of Cr sites and occupations of Cr( $12k$ ), Cr( $2a$ ), and Cr( $4f_{vi}$ ) sites from neutron refinement.  $J$  and  $\varepsilon$  are the couplings extracted from the high- $T$  mean-field analysis for the three samples.

## REFERENCES

- [1] P. Schiffer and A. P. Ramirez, Comments Condens. Matter Phys. **18**, 21 (1996) and ref. therein.
- [2] C. Broholm, G. Aeppli, G. P. Espinosa, and A. S. Cooper, Phys. Rev. Lett. **65**, 3173 (1990); C. Mondelli, K. Andersen, H. Mutka, C. Payen, B. Frick, Physica B **267-268**, 139 (1999).
- [3] S.-H. Lee *et al.*, Phys. Rev. Lett. **76**, 4424 (1996).
- [4] P. Schiffer and I. Daruka, Phys. Rev. B **56**, 13 712 (1997).
- [5] P. Mendels *et al.*, *Cond-mat* 0004077; P. Mendels *et al.*, invited paper.
- [6] L. Limot *et al.*, in preparation.
- [7] A. P. Ramirez, G. P. Espinosa, and A. S. Cooper, Phys. Rev. Lett. **64**, 2070 (1990); B. Martinez *et al.*, Phys. Rev. B **46**, 10 786 (1992).
- [8] A. Keren *et al.*, Phys. Rev. B **57**, 10 745 (1998).
- [9] W. G. Clark, M. E. Hanson, and F. Lefloch, Rev. Sci. Instrum. **66**, 2453 (1995).
- [10] K. Motida and S. Miahara, J. Phys. Soc. Jpn. **33**, 687 (1972).
- [11] H. Ohta *et al.*, J. Phys. Soc. Jpn. **65**, 848 (1996).
- [12] E. J. Samuelsen *et al.*, Physica **48**, 13 (1970).

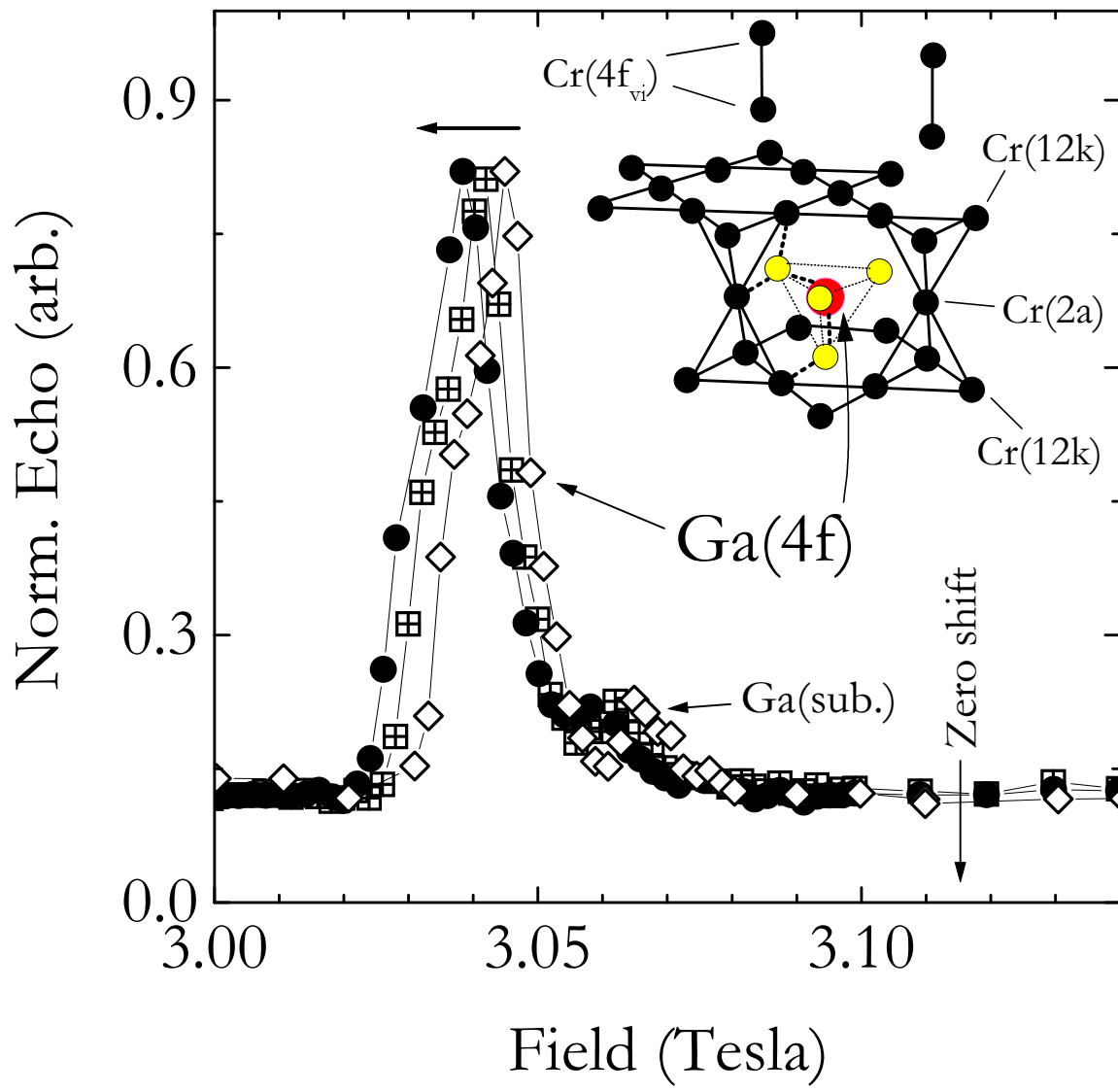
## FIGURES

FIG. 1. Typical  $^{71}\text{Ga}$  field sweep obtained at 40.454 MHz for  $p = .96$ . From right to left: 150 K, 120 K, 100 K. The zero shift reference position is 3.116 Tesla. Horizontal arrow indicates shift direction upon cooling. Inset: Crystal structure of ideal  $\text{SrCr}_9\text{Ga}_3\text{O}_{19}$ . The thick dashed lines show the hyperfine coupling paths of  $\text{Ga}(4f)$  nucleus to frustrated Cr moments. Light grey circles are oxygens.  $\text{Cr}(12k)$  are arranged to form a distorted kagomé network and are coupled through  $\text{Cr}(2a)$ . The full structure is  $\text{Cr}(4f_{vi})\text{--Cr}(4f_{vi})/\text{kagomé-Cr}(2a)\text{-kagomé/Cr}(4f_{vi})\text{--Cr}(4f_{vi})$ , etc.

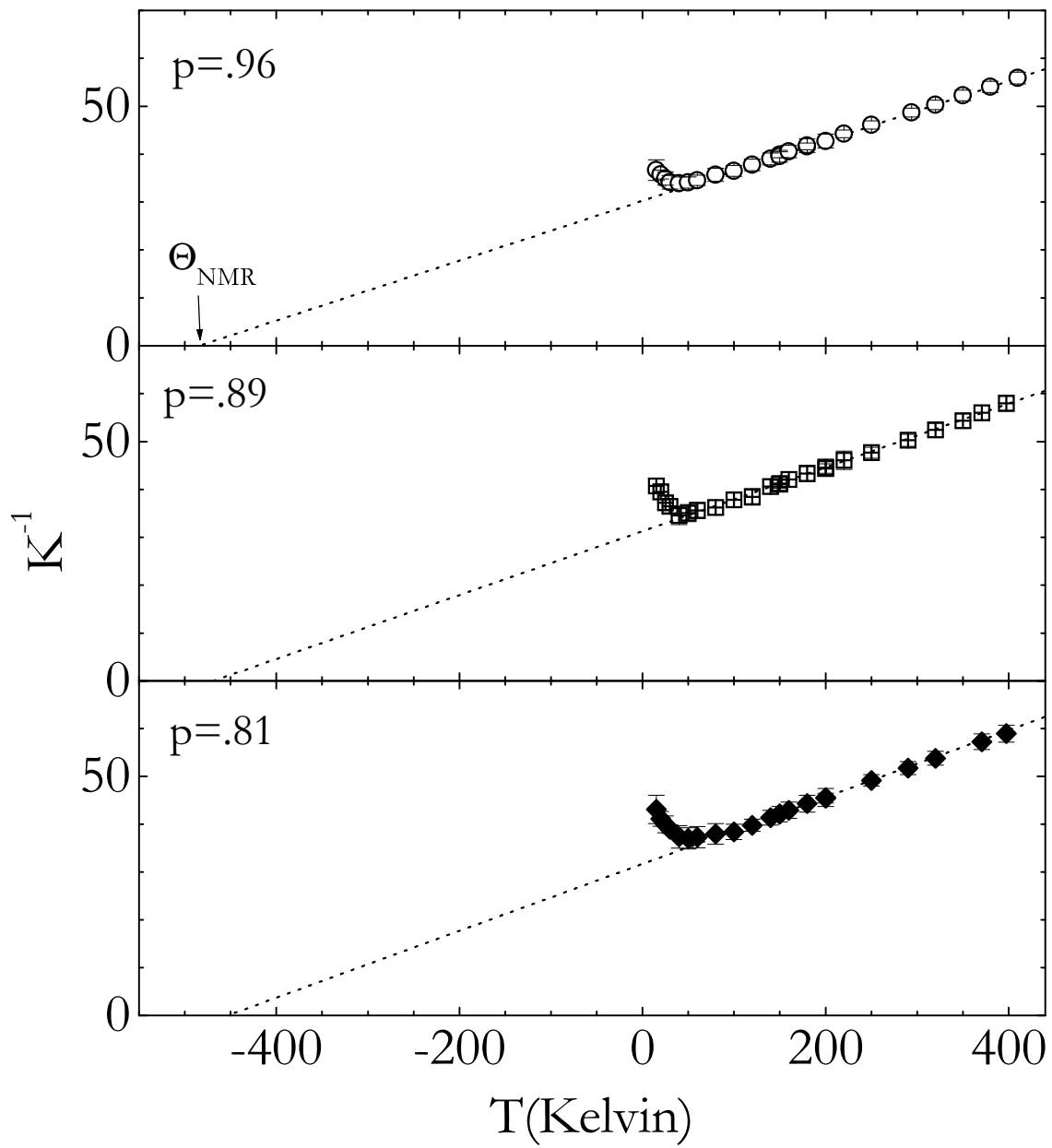
FIG. 2.  $K^{-1}$  versus  $T$  down to 15 K, for all samples. Minor second-order quadrupole corrections have been performed. The straight line extrapolation of  $K^{-1} = 0$  yields  $\Theta_{NMR}$ .

FIG. 3. Calculated mean-field susceptibilities  $\chi_{12k}$  and  $\chi_{2a}$  of the  $\text{Cr}(12k)$  and  $\text{Cr}(2a)$  moments versus  $T$ , with increasing  $\text{Cr}(2a)\text{--Cr}(12k)$  coupling.  $J$  is fixed to 85 K and  $p_{12k} = p_{2a} = 1$ .

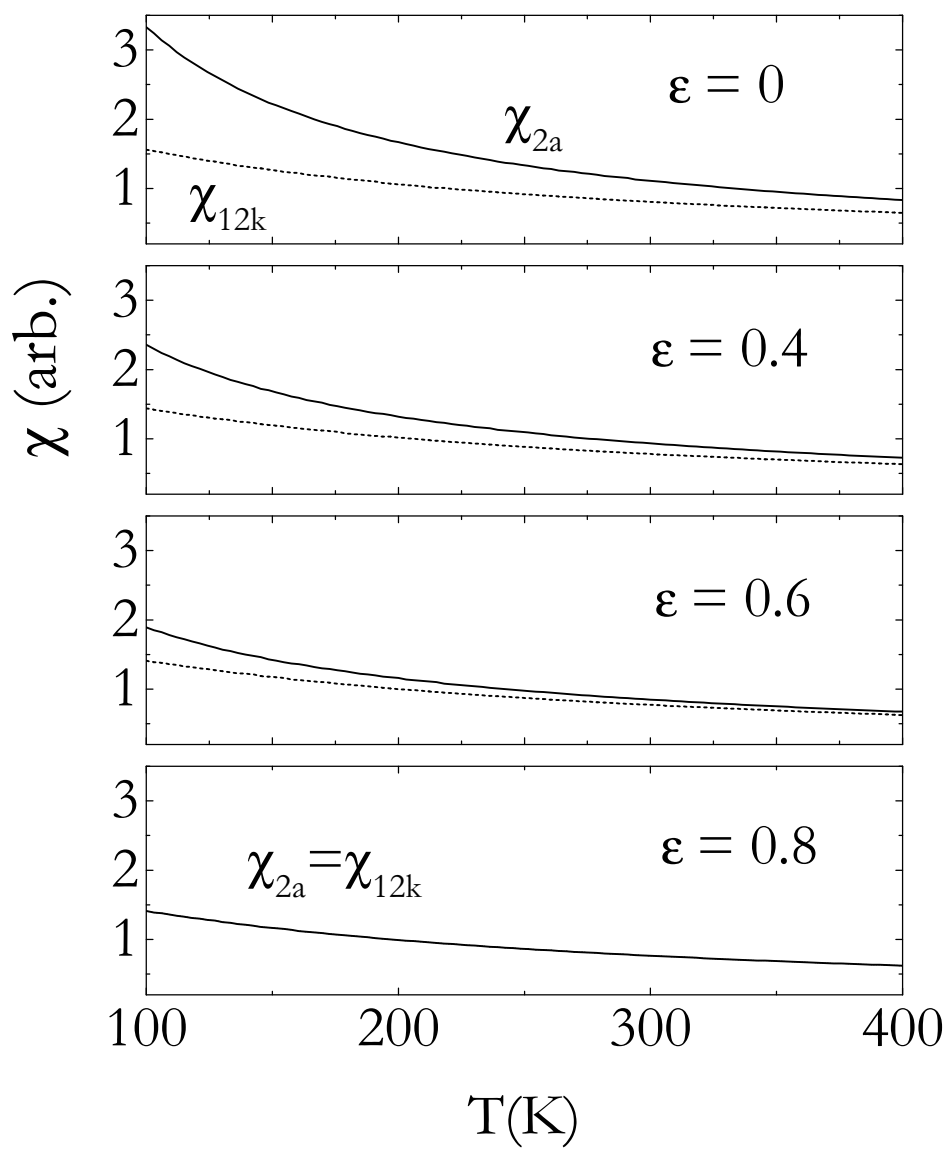
FIG. 4. The  $(\varepsilon, J, \delta)$  set of values which reproduce the linear variation of  $K^{-1}$  with  $T$  of the  $p = .96$  sample. For a given value of  $\varepsilon$  (abscissa) there is an associated value  $\delta$  (upper panel) and  $J$  (bottom panel).



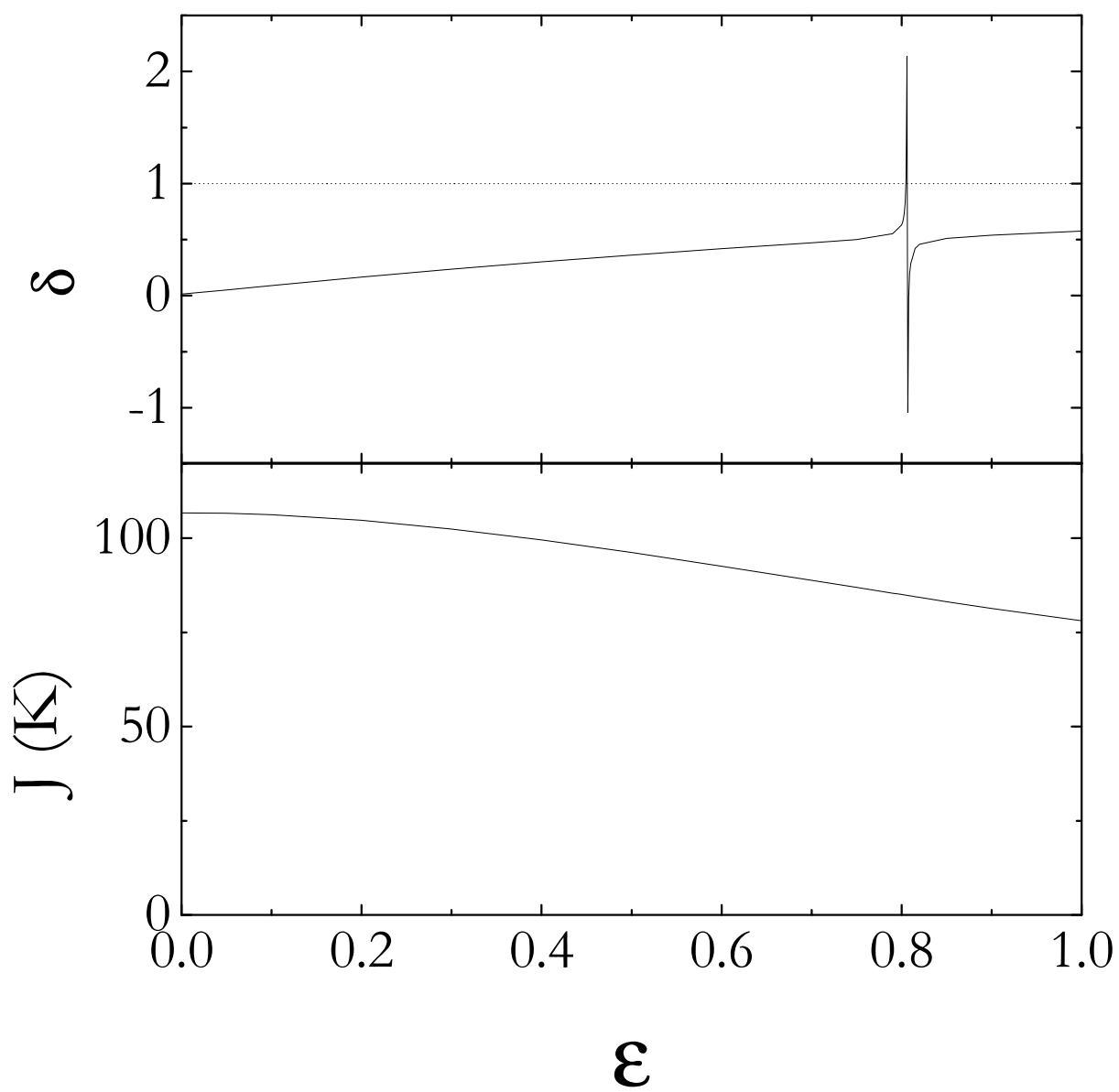
Limot et al., Fig.1



Limot et al., Fig.2



Limot et al., Fig.3



Limot et al., Fig.4